



# Improved resonance calculation of fluoride salt-cooled high-temperature reactor based on subgroup method



Qingming He, Liangzhi Cao, Hongchun Wu, Tiejun Zu \*

School of Nuclear Science and Technology, Xi'an Jiaotong University, Xi'an, Shaanxi 710049, China

## ARTICLE INFO

### Article history:

Received 10 June 2015

Received in revised form 7 November 2015

Accepted 9 November 2015

Available online 28 November 2015

### Keywords:

Subgroup method

Resonance elastic scattering effect

Resonance interference effect

Double heterogeneity

## ABSTRACT

The subgroup method is improved in several aspects to address challenges brought on by design features of the Fluoride salt-cooled High-temperature Reactor (FHR). Firstly, the Dancoff correction is applied to resolve the double heterogeneity arising from embedding TRISO fuel particles in the matrix of pebbles. Secondly, a fast Resonance Interference Factor (RIF) scheme is proposed to treat the resonance interference effect in the FHR. In this scheme, the heterogeneous system is converted into a homogeneous one according to self-shielded cross section conservation of the dominant resonant nuclide. The resonance interference effect is considered in the equivalent homogenous system by correcting the non-interfered self-shielded cross sections with RIFs which are obtained by solving the slowing down equation in hyper-fine energy group ( $\sim 1\text{M}$  number of energy groups). Finally, the resonance elastic scattering effect becomes considerable due to high temperatures in the FHR. This effect is considered by substitution of the conventional Resonance Integral (RI) table with that generated by the Monte Carlo method. The Monte Carlo method is modified via the Doppler Broadening Correction Rejection (DBRC) method to implement the Doppler broadened scattering kernel. The numerical results show that the Dancoff correction can significantly reduce errors brought about by the double heterogeneity. The fast RIF scheme provides more accurate effective self-shielded cross sections than the conventional iteration scheme. In addition, the speedup ratio of the fast RIF scheme is  $\sim 3.3$  compared with the conventional on-the-fly RIF schemes for TRU TRISO. The scheme to generate RI table can resolve the resonance elastic scattering effect encountered by the conventional scheme.

© 2015 Elsevier Ltd. All rights reserved.

## 1. Introduction

The subgroup method (Nikolaev et al., 1971; Chiba and Unesaki, 2006; Hébert, 2009) has long been used for resonance calculations and is widely employed in neutron transport codes such as HELIOS (Stamm'ler, 2001), DeCART (Joo et al., 2004) and MPACT (Liu et al., 2013a) for its geometrical flexibility. In the subgroup method, the fluctuation of the cross sections is described by a probability table, including subgroup cross sections and the corresponding subgroup probabilities. The probability table is then used to formulate the subgroup fixed source problem (SFSP). The SFSP can be solved by multi-group transport methods such as the Method Of Characteristics (MOC) (Chen et al., 2008; Zhang et al., 2011) to obtain the subgroup flux which is then used to weight the subgroup cross sections and obtain the effective self-shielded cross sections.

The FHR is a novel reactor concept that combines High Temperature Reactor (HTR) fuel and flibe ( ${}^7\text{LiF}-\text{BeF}_2$ ) coolant (Kim et al.,

2003; Fratoni, 2008; Li et al., 2015). It is a promising concept to overcome the drawbacks of the Very High Temperature Reactor (VHTR) such as low power density and high pressure of coolant. However, the design of the FHR challenges the conventional subgroup method. Firstly, the pebble fuel element comprised of an outer fuel-free graphite spherical shell and a fuel zone is used in the FHR. In the fuel zone of a pebble, tens of thousands of TRISO particles are embedded in a graphite matrix. This system can be considered as a double heterogeneous system (Tsuchihashi et al., 1985) where resonance calculation methods such as equivalence theory and subgroup method cannot be directly applied. Secondly, the fuel enrichment of the FHR is typically higher than that of the Pressurized Water Reactor (PWR), which will introduce complex resonance interference effects (Wehlage et al., 2005). Besides, in recent study, the  $\text{TRUO}_{1.7}$  fuel is used in the FHR to incinerate transuranic (TRU) elements including Plutonium, Americium, Neptunium, Curium and so on (Fratoni, 2008). This kind of fuel mixture has a complex composition and challenges the conventional method to treat resonance interference effects. Finally, the FHR features high temperatures up to  $1000\text{ }^\circ\text{C}$  which makes the

\* Corresponding author. Tel.: +86 029 82663285; fax: +86 029 82667802.

E-mail address: [tiejun@mail.xjtu.edu.cn](mailto:tiejun@mail.xjtu.edu.cn) (T. Zu).

resonance elastic scattering effect significant (Becker et al., 2009a). The conventional scheme, generating the Resonance Integral (RI) table by solving the slowing down equations over a range of background cross sections based on asymptotic scattering kernel (MacFarlane, 2000), will introduce considerable errors due to underestimation of neutron up-scattering at high temperatures (Ouisloumen and Sanchez, 1991). This paper will focus on these significant effects of double heterogeneity, resonance interference and resonance elastic scattering, for the FHR.

A pile of pebbles in FHR can be considered as a double heterogeneous system (Sanchez and Masiello, 2002). The first heterogeneity comes from the heterogeneity of the TRISO particle and the surrounding graphite matrix. The second heterogeneity is from the heterogeneity of the fuel zone and the graphite spherical shell. The Dancoff factor has long been used for consideration of the double heterogeneity effect in the HTR (Hyun et al., 2010; Kloosterman and Ougouag, 2007; Kloosterman et al., 2005). The typical Dancoff correction considers two steps. In the first step, the coated TRISO particle with its surrounding matrix is modeled as a one-dimensional sphere with its self-shielded cross sections calculated by the subgroup method. In the second step, the infinite-medium Dancoff factor and the double heterogeneous Dancoff factor are calculated. The Dancoff factors are used to correct the self-shielded cross sections obtained in the first step. The infinite-medium Dancoff factor accounts for the probability that a neutron escaping from a fuel kernel enters another fuel kernel within an infinite-medium fuel zone without colliding with a moderator nucleus. The double heterogeneous Dancoff factor is the probability that a neutron escaping from a fuel kernel enters another fuel kernel within the same pebble or another pebble without colliding with a moderator nucleus. In this paper, the analytical scheme proposed by Bende (Bende and Hogenbirk, 1999) is applied to calculate the Dancoff factors.

The resonance interference effect is caused by the fact that the multi-group nuclear data is prepared for each nuclide ignoring the overlap of the resonance peaks of different nuclides. The interference effect is conventionally treated by iteration, where, when the present resonant nuclide is treated, all the other ones are assumed to be without resonance peaks (Askew et al., 1966). However, there exist two shortcomings in this scheme. Firstly, the iteration procedure is time-consuming especially when there are numerous resonant nuclides due to burn-up. Secondly, the results of iteration cannot converge to the true value (Williams, 1983). To speed up the iteration procedure, a Resonant Nuclide Grouping (RNG) scheme was proposed (Stamm'ler, 2001). In this scheme, numbers of resonant nuclides are grouped into a small number of categories according to their resonance features. Although this scheme can improve the calculation efficiency, it suffers from loss of precision. To gain higher precision, a RIF scheme was developed (Wehlage et al., 2005; Williams, 1983). The RIF is the quotient of two sets of self-shielded cross sections, that is, the self-shielded cross sections with a single resonant nuclide and the self-shielded cross sections with the mixture of all nuclides. These self-shielded cross sections are calculated in continuous energy or hyper-fine energy groups. Then the RIF is applied to the self-shielded cross sections without resonance interference obtained by the subgroup method. The RIFs can be calculated in priori and tabulated (Kim and Hong, 2011; Peng et al., 2013), or be generated on-the-fly (Kim and Williams, 2012; Liu et al., 2013b) for each resonant nuclide. However, this scheme increases the storage of nuclear data and the conventional on-the-fly scheme increases the computation time. In this paper, in order to treat resonance interference effect efficiently and accurately, a fast RIF scheme is proposed. For each resonance group, the dominant resonant nuclide is selected. The self-shielded cross sections of the dominant resonant nuclide without resonance interference are

calculated by the subgroup method. Then the heterogeneous system is converted to a homogeneous one by preserving the self-shielded cross section of the dominant nuclide. Finally, the self-shielded cross sections of all the resonant nuclides with resonance interference are obtained by solving the homogeneous slowing down problem.

In the subgroup method, the probability table is generated by fitting Resonance Integral (RI) tables. Methods such as the hyper-fine energy group method and the Monte Carlo method are often used to solve the slowing down problems over a range of background cross sections to generate the RI tables (Joo et al., 2009; Kim and Hong, 2011; Kim et al., 2003). For the hyper-fine energy group method, the asymptotic elastic scattering kernel assuming that the target nucleus is at rest is adopted (Ishiguro and Takano, 1971; Leszczynski, 1987; MacFarlane, 2000). For the Monte Carlo method, the scattering kernel without Doppler broadening assuming that the scattering cross sections at zero temperature are constant in energy is adopted (X-5 Monte Carlo Team, 2003). However, when the neutron energy is in the vicinity of the elastic scattering resonance peaks in the epithermal energy range, the thermal motion of the target will considerably influence the elastic scattering reaction and increase neutron capture in the resonance peaks. As a consequence, the eigenvalue and the Fuel Temperature Coefficient (FTC) are affected. This effect is the so-called resonance elastic scattering effect (Lee et al., 2008). Recent works have demonstrated that the resonance elastic scattering effect on eigenvalues is  $\sim 200$  pcm at hot full power for light water reactor (LWR) (Lee et al., 2008) and  $\sim 400$  pcm for Very High Temperature Reactor (VHTR) (Becker et al., 2009b). It is also shown that the Fuel Temperature Coefficients (FTC) are affected by  $\sim 10\%$  for LWR (Ono et al., 2012). To take into account this effect in the deterministic method, Lee et al. utilized Monte Carlo method, which considers resonance elastic scattering effect via Weight Correction Method (WCM), to generate RI tables (Lee et al., 2008). Ono et al. implemented the simplified resonance elastic scattering model in the GROUPT module of NJOY (Ono et al., 2012). Mao et al. combined the RIF method and the Improved Méthode Direct (IMD) method to treat the resonance interference effect and the resonance elastic scattering effect simultaneously (Mao et al., 2015). In this paper, to introduce Doppler broadened scattering kernel for the multi-group deterministic method, the scattering kernel of the Monte Carlo code OpenMC (Romano and Forget, 2013) is modified via DBRC to generate RI table. The improved RI table is combined with the subgroup method to recover the resonance elastic scattering effect in the FHR.

The above improvements are implemented on a subgroup method based code named SUGAR (Cao et al., 2011; He et al., 2014). The theory and model of the subgroup method, the Dancoff correction for double heterogeneity, the schemes for treating resonance interference effect and the resonance elastic scattering correction are described in Section 2. The numerical results and analysis are provided in Section 3. The summations and conclusions are given in the last section.

## 2. Theory and model

### 2.1. Subgroup method

As illustrated in Fig. 1, subgroups are defined according to the magnitude of the cross section rather than the energy in a broad energy group. The energy range of a subgroup is defined by

$$\Delta E_{g,i} \in \{E | \sigma_{g,i} < \sigma(E) \leq \sigma_{g,i+1}\} \quad (1)$$

where  $g$  is the energy group index and  $i$  is the subgroup index.

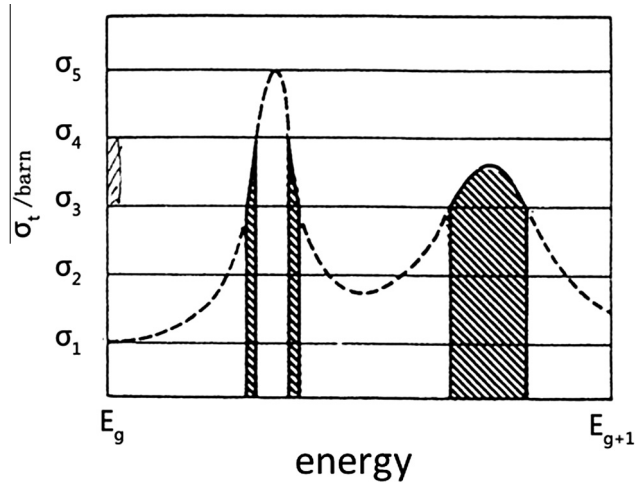


Fig. 1. Definition of subgroups in a broad energy group.

The subgroup cross section and the subgroup probability are respectively defined as

$$\sigma_{x,g,i} = \frac{\int_{\Delta E_{g,i}} \sigma_x(E) \phi(E) dE}{\int_{\Delta E_{g,i}} \phi(E) dE} \quad (2)$$

$$p_{g,i} = \frac{\Delta E_{g,i}}{\Delta E_g} \quad (3)$$

where, subscript “x” is the type of the cross sections of the subgroup cross section. The probability table is obtained by preserving self-shielded cross sections over a range of dilution cross sections (Cao et al., 2011).

According to the definition of the subgroup, the equation of the SFSP can be obtained by integration of the continuous-energy Boltzmann transport equation over a subgroup

$$\Omega \nabla \phi_{g,i}(\mathbf{r}, \Omega) + \Sigma_{t,g,i}(\mathbf{r}) \phi_{g,i}(\mathbf{r}, \Omega) = Q_{s,g,i}(\mathbf{r}, \Omega) + Q_{f,g,i}(\mathbf{r}, \Omega) \quad (4)$$

where  $\phi_{g,i}(\mathbf{r}, \Omega)$  is the subgroup flux;  $\Sigma_{t,g,i}(\mathbf{r})$  is the macro total subgroup cross section;  $Q_{s,g,i}(\mathbf{r}, \Omega)$  and  $Q_{f,g,i}(\mathbf{r}, \Omega)$  are the scattering source and the fission source in the subgroup respectively. The fission source in the resonance energy range is so small that it can be ignored. The scattering source is written as

$$Q_{s,g,i}(\mathbf{r}, \Omega) = p_{g,i} \sum_{g'} \int_{\Delta E_{g'}} dE' \int_{\Delta E_{g,i}} dE \int_{4\pi} d\Omega' \Sigma_s(\mathbf{r}; E', \Omega' \rightarrow E, \Omega) \phi(E', \mathbf{r}, \Omega') \quad (5)$$

where  $\Sigma_s(\mathbf{r}; E', \Omega' \rightarrow E, \Omega)$  is the scattering cross section. Since Eq. (4) has the same form as the multi-group transport equation, it can be solved by employing mature multi-group transport solvers. In this paper, ANISN (Engle, 1967) is used to solve the one-dimensional problems and a Matrix Method of Characteristics solver MMOC (Zhang et al., 2011) for the two-dimensional problems. After the subgroup flux is obtained, the effective self-shielded cross sections can be calculated by

$$\sigma_{x,g}^{\text{eff}}(\mathbf{r}) = \frac{\int_{4\pi} \sum_i \sigma_{x,g,i}(\mathbf{r}) \phi_{g,i}(\mathbf{r}, \Omega) d\Omega}{\int_{4\pi} \sum_i \phi_{g,i}(\mathbf{r}, \Omega) d\Omega} \quad (6)$$

Generally, the RI table is prepared by solving slowing down problems over a range of background cross sections. Then, the self-shielded cross sections over a range of dilution cross sections are calculated from the RI table as follows

$$\sigma_{x,g}(\sigma_0) = \frac{\sigma_b \text{RI}_{x,g}(\sigma_b)}{\sigma_b - \text{RI}_{a,g}(\sigma_b)} \quad (7)$$

$$\sigma_b = \sigma_0 + \lambda \sigma_p, \quad (8)$$

where  $\sigma_p$  is the potential scattering cross section;  $\sigma_0$  is the dilution cross section;  $\lambda$  is the Goldstein–Cohen factor;  $\sigma_b$  is the background cross section. Both of the RI table and self-shielded cross section table are used in the subgroup method presented in this paper.

## 2.2. Dancoff correction for double heterogeneity

A pile of pebbles can be recognized as a double heterogeneous system. To treat the double heterogeneity with the subgroup method, Dancoff correction is introduced.

To treat the first heterogeneity, an equivalent one-dimensional spherical shell model with a white boundary is built based on conservation of volume. This model can be also considered as an approximation for a random distribution of TRISO particles in an infinite fuel zone of pebbles. The self-shielded cross sections are obtained through subgroup resonance calculation based on this model.

To treat the second heterogeneity, two sets of Dancoff factors, namely the infinite medium Dancoff factor and the double heterogeneous Dancoff factor, are calculated. And then the self-shielded cross sections obtained in the first step are corrected according to

$$\sigma_{k,x,g}^{\text{eff}} = \sigma_{k,x,g}^{\infty} \frac{\sigma_{k,x,g} [\sigma_{0,f,k} + (1 - C_{d,g}) \sigma_{e,k,g}]}{\sigma_{k,x,g} [\sigma_{0,f,k} + (1 - C_{\infty,g}) \sigma_{e,k,g}]} \quad (9)$$

$$\sigma_{0,f,k} = \sum_{k' \neq k} N_{k'} \lambda_{k'} \sigma_{p,k'} / N_k, \quad (10)$$

where  $\sigma_{k,x,g}^{\infty}$  is the self-shielded cross section in an infinite fuel zone calculated in the first step;  $C_{\infty,g}$  is the infinite medium Dancoff factor;  $C_{d,g}$  is the double heterogeneous Dancoff factor;  $\sigma_{0,f,k}$  is the part of the background cross section that is contributed by all nuclides except the currently calculated resonant nuclide;  $\sigma_{k,x,g}(\sigma_0)$  is the self-shielded cross section table;  $\sigma_{e,k,g}$  can be estimated according to the equivalence relationship as follows

$$\sigma_{k,x,g}^{\infty} = \sigma_{k,x,g} [\sigma_{0,f,k} + (1 - C_{\infty,g}) \sigma_{e,k,g}] \quad (11)$$

The analytical method based on a spherical two-region model is applied to calculate the Dancoff factors (Bende and Hogenbirk, 1999; Talamo, 2007).

## 2.3. Resonance interference

### 2.3.1. Iteration scheme

The resonance interference effect is caused by ignoring the overlap of resonance peaks of different nuclides, when the multi-group nuclear data is generated. Conventionally, the effect is treated by an iteration scheme (Askew et al., 1966). In fact, for the subgroup method, an assumption that there is only one resonant nuclide in the medium is made in Eq. (4). An iteration scheme within a broad energy group is carried out as follows:

- (1) Take nuclide  $k$  as the present resonant nuclide with all the others being assumed to be without resonance peaks. Calculate the macro subgroup cross sections of the medium as follows

$$\Sigma_{x,g,i} = N_k \sigma_{x,k,g,i} + \sum_{k' \neq k} N_{k'} \sigma_{x,k',g} \quad (12)$$

For nuclides without intrinsic resonance peaks, the micro cross sections  $\sigma_{x,k',g}$  are directly read from the multi-group nuclear data library. For resonant nuclides assumed to be without resonance peaks, the micro cross sections are guessed values at the first iteration step or updated values

from the previous iteration. Solve Eq. (4) to obtain the subgroup flux and calculate the self-shielded cross sections of the present nuclide given by Eq. (6).

- (2) Carry out the first step for the next resonance nuclide.
- (3) After sweeping all the resonant nuclides, perform a convergence test for the self-shielded cross sections. If the self-shielded cross sections are converged, the iteration is over; otherwise perform another sweep from the first step.

There are two main drawbacks for the iteration scheme. Firstly, it is time-consuming due to the iteration and convergence test. Secondly, it has been proved that there are cases where the iteration scheme cannot give the correct results (Williams, 1983).

### 2.3.2. RNG scheme

The first drawback of the iteration scheme becomes acute for cases with numerous nuclides existing in the fuel region. To handle these cases, the RNG scheme is applied in codes such as HELIOS (Stamm'ler, 2001) and SUGAR (He et al., 2014). The basic idea is that the numerous resonant nuclides are grouped into a small number of categories according to the resonance features. A category of resonant nuclides can be considered as a pseudo nuclide, whose subgroup cross section can be calculated as

$$\sigma_{l,x,i} = \frac{\sum_{k \in C_l} N_k \sigma_{x,k,i}}{\sum_{k \in C_l} N_k} \approx \frac{\sum_{k \in C_l} N_k \frac{RI_{k,\infty}}{RI_{\text{typical},\infty}} \sigma_{x,\text{typical},i}}{\sum_{k \in C_l} N_k} \quad (13)$$

The density of the pseudo nuclide is

$$N_l = \sum_{k \in C_l} N_k \quad (14)$$

where,  $l$  is the category index;  $C_l$  is the collection of the nuclide indexes of the category  $l$ ;  $RI_{k,\infty}$  is the RI at infinite dilution; the subscript "typical" stands for the typical resonant nuclide of the category. The typical nuclide is the nuclide with the maximum atomic density in the category. After grouping the resonant nuclides into several categories, the iteration scheme described previously is carried out for the pseudo nuclides. The estimated subgroup flux is used to calculate the self-shielded cross sections of the typical nuclide according to Eq. (6). The self-shielded cross sections of the atypical nuclides are given by

$$\sigma_{x,k} = \frac{RI_{k,\infty}}{RI_{\text{typical},\infty}} \sigma_{\text{typical},x} \quad (15)$$

In practice, all the resonant nuclides are classified into two or three categories so that the computation time will be reduced greatly, even when there are tens of resonant nuclides for burn-up cases. However, this scheme is still based on the iteration scheme and the resonance interference among the categories is poorly treated; besides, the interference among nuclides within a same category is not considered at all. Therefore, the precision of this scheme is questionable.

### 2.3.3. Conventional RIF scheme

It has been proved that the RIF scheme has higher precision than the iteration scheme (Wehlage et al., 2005; Williams, 1983). In the RIF scheme, two sets of self-shielded cross section are calculated for each nuclide. One set is calculated with a single resonant nuclide; the other set is calculated by considering the entire mixture of all the resonant nuclides. The correction equation for the self-shielded cross section is

$$\sigma_{x,k,g}^{\text{eff}} = \sigma_{x,k,g} \text{RIF}_{x,k,g} = \sigma_{x,k,g} \frac{\sigma_{x,k,g}^{\text{all}}}{\sigma_{x,k,g}^{\text{single}}} \quad (16)$$

where  $\text{RIF}_{x,k,g}$  is the resonance interference factor.

The RIFs can be calculated in a homogeneous system or a heterogeneous system. The latter was realized by CHIBA (CHIBA, 2003) who employed PEACO (Ishiguro and Takano, 1971) to calculate the RIFs in a pin cell model. However, the heterogeneous model shows no advantage over the homogeneous one in terms of precision, but consumes more computational resources (Kim and Williams, 2012). Therefore, here, we will consider the homogeneous model only.

Although the homogeneous model is faster than the heterogeneous one, it still represents a computational drain. Much work has been done to improve the computation efficiency of the RIF scheme, such as the "cross-shielded  $f$ -factors" (R B Kidman et al., 1970) and the tabulated RIFs (Kim and Hong, 2011; Peng et al., 2013). Although the implementation of these schemes are different, the basic idea is the same. In these schemes, the RIFs are tabulated as a function of the temperature, dilution cross section and an enrichment-type variable. The tabulation scheme is easily applied to cases where there are only two resonant nuclides contained in the fuel, however, it may cause a storage problem for burn-up cases or MOX fuel where there are more than two resonant nuclides to be considered.

In this paper, to combine the subgroup method with the RIF scheme, the self-shielded cross section without resonance interference of the resonant nuclides are obtained by the solution of Eq. (4). When one resonant nuclide is treated, all the other ones are considered as background nuclides. The cross sections of the background nuclides are given by

$$\sigma_{t,g,k} = \sigma_{s,g,k} = \sigma_{p,k} \quad (17)$$

$$\sigma_{a,g,k} = 0, \quad (18)$$

where  $\sigma_{t,g,k}$ ,  $\sigma_{s,g,k}$ ,  $\sigma_{p,k}$  and  $\sigma_{a,g,k}$  are the total cross section, scattering cross section, potential scattering cross section and absorption cross section respectively. Once the self-shielded cross sections are obtained, the equivalent dilution cross sections are determined by interpolation in the self-shielded cross section table. Then, the RIFs are calculated by solving the equivalent homogeneous slowing down problems on the fly and applied to determine the self-shielded cross sections according to Eq. (16).

### 2.3.4. Fast RIF scheme

To overcome the drawbacks of the conventional RIF schemes, an improvement scheme named fast RIF is proposed. For a heterogeneous system, the calculation flow is as follows

- (1) For each energy group, a dominant resonant nuclide is chosen according to the magnitude of  $RS_{k,g} = N_k RI_{t,k,g}^{\text{max}} / RI_{t,k,g}^{\text{min}}$ . The  $RI_{t,k,g}^{\text{max}}$  and  $RI_{t,k,g}^{\text{min}}$  are the maximum total RI and minimum total RI of group  $g$  in the RI table of nuclide  $k$ , respectively. The quotient of these two values represent the intensity of the resonance in the microscopic scale and the  $RS_{k,g}$  represents the intensity in the macroscopic scale.
- (2) Eq. (4) is solved for the dominant resonant nuclide for each energy group, with all the other resonant nuclides considered as background nuclides. After the subgroup flux is obtained, the self-shielded cross section of the dominant resonant nuclide is obtained according to Eq. (6).
- (3) The heterogeneous system is converted to an equivalent homogeneous system according to self-shielded cross section conservation of the dominant resonant nuclide. The densities of the resonant nuclides of the homogeneous system are the same as those of the heterogeneous system. The equivalent macroscopic dilution cross section is given by

$$\Sigma_{0,g} = \sigma_{0,g} N_{\text{dom}} - \sum_{k' \neq \text{dom}} \sigma_{p,k'} N_{k'}, \quad (19)$$

where  $\sigma_{0,g}$  is the equivalent microscopic dilution cross section which is obtained by interpolation in the self-shielded cross sections table of the dominant resonant nuclide. The subscript “dom” stands for the dominant resonant nuclide and  $N_{\text{dom}}$  is the atomic density of the dominant nuclide.  $\sigma_{p,k'}$  and  $N_{k'}$  are the potential scattering cross section and the atomic density of nuclides other than the dominant one.

- (4) The constructed homogeneous problem is solved with RMET21 (Leszczynski, 1987) based on the hyper-fine energy group method and the effective self-shielded cross sections of all the resonant nuclides are obtained.

In a heterogeneous system, if the number of resonant nuclides is  $K$ , the number of spatial mesh with resonance nuclides is  $M$  and the number of the resonance groups is  $G$ , then the number of SFSPs to be solved is  $G$  and the number of the slowing down calculations is  $M$  for the fast RIF scheme. While for the conventional RIF scheme, the number for the above two kinds of calculations are  $K \times G$  and  $K \times M$ , respectively. Therefore, the speedup ratio of the fast RIF scheme can be estimated as

$$a = \frac{K \times G \times T_{\text{SFSP}} + K \times M \times T_{\text{SDP}}}{G \times T_{\text{SFSP}} + M \times T_{\text{SDP}}} \quad (20)$$

where  $T_{\text{SFSP}}$  is the time to solve the SFSP and  $T_{\text{SDP}}$  is the time to solve the slowing down problem.

#### 2.4. Resonance elastic scattering

According to the above discussions, the RI table is an important data base for the subgroup method. Generally, the RI table is generated using hyper-fine group method (Joo et al., 2009; Kim and Hong, 2011) or the Monte Carlo method (Kim et al., 2003). When the RI table is generated with hyper-fine group method, the asymptotic scattering kernel, assuming that the target is at rest in the collision with a neutron, is conventionally adopted in the slowing down equation (MacFarlane, 2000). In the Monte Carlo method, the free gas model is used to consider the thermal motion of target. In this model, the variation of the scattering cross section with target velocity is ignored (X-5 Monte Carlo Team, 2003). These assumptions underestimate the up-scattering of neutron in the vicinity of resonance peaks which in turn affect the eigenvalues and FTC (Lee et al., 2008). Previous research has proven that the above mentioned assumptions can introduce considerable effect on the neutronics calculations (Becker et al., 2009b; Kim and Hartanto, 2012; Lee et al., 2008; Ouisloumen and Sanchez, 1991). The conventional asymptotic scattering kernel and free gas model are illustrated in Sections 2.4.1 and 2.4.2 and then the DBRC method (Becker et al., 2009b) is introduced to consider the resonance elastic scattering effect in Section 2.4.3.

##### 2.4.1. The asymptotic scattering kernel

The neutron slowing down equation for a homogeneous system is

$$\sum_k \Sigma_{t,k}(E) \phi(E) = \sum_k \int_0^\infty \Sigma_{s,k}(E) f_k(E' \rightarrow E) \phi(E') dE' \quad (21)$$

where  $k$  is the nuclide index;  $f_k(E' \rightarrow E)$  is the scattering kernel. Conventionally, the target is assumed to be at rest and the asymptotic scattering kernel is adopted

$$f_k(E' \rightarrow E) = \frac{1}{(1 - \alpha_k)E'} \quad (22)$$

where  $\alpha_k = (A_k - 1)^2 / (A_k + 1)^2$  and  $A_k$  is the mass ratio of the target to a neutron.

##### 2.4.2. The free gas model

The Monte Carlo method employs the free gas model to take into account the thermal motion of the target. To determine the velocity of the out-going neutron in a collision with a target, the velocity of the target is sampled at first. The probability density function of the target velocity is

$$P(V, \mu | v_n) = \frac{\sigma_s(v_r, 0) v_r P(V)}{2\sigma_s^{\text{eff}}(v_n, T) v_n} \quad (23)$$

where  $V$  is the speed of the target;  $\mu$  is the cosine of the scattering angle;  $v_n$  is the speed of the neutron;  $v_r$  is the relative speed;  $T$  is the temperature of the medium;  $P(V)$  is the Maxwell-Boltzmann distribution;  $\sigma_s(v_r, 0)$  is the elastic scattering cross section at relative speed at zero temperature;  $\sigma_s^{\text{eff}}(v_n, T)$  is the effective elastic scattering cross section. Assuming that the elastic scattering cross section at zero temperature doesn't vary with the target velocity (X-5 Monte Carlo Team, 2003), Eq. (23) can be written as

$$P(V, \mu | v_n) = C \left\{ \frac{v_r}{v_n + V} \right\} \{P_1 f_1(V) + P_2 f_2(V)\}, \quad (24)$$

where

$$C = \frac{(2 + \sqrt{\pi} \beta v_n) \sigma_s(v_r, 0)}{2\sigma_s^{\text{eff}}(v_n, T) \sqrt{\pi} \beta v_n} \quad (25)$$

$$P_1 = \frac{1}{1 + \frac{\sqrt{\pi} \beta v_n}{2}} \quad (26)$$

$$P_2 = 1 - P_1 \quad (27)$$

$$f_1(V) = 2\beta^4 V^3 e^{-\beta^2 V^2} \quad (28)$$

$$f_2(V) = \frac{4\beta^3}{\sqrt{\pi}} V^2 e^{-\beta^2 V^2} \quad (29)$$

$$\beta = \sqrt{\frac{AM_n}{2kT}} \quad (30)$$

$M_n$  is the mass of neutron and  $k$  is the Boltzmann constant.

Note that this assumption is valid for light nucleus such as  $^1\text{H}$  but not for heavy nucleus such as  $^{238}\text{U}$  which has elastic resonance peaks in the epithermal energy range.

##### 2.4.3. The DBRC method

The DBRC method is introduced to take into account the thermal motion and the energy-dependent elastic scattering cross section. The modified probability density function can be written as

$$P(V, \mu | v_n) = C' \left\{ \frac{\sigma_s(v_r, 0)}{\sigma_s^{\text{max}}(v_\xi, 0)} \right\} \left\{ \frac{v_r}{v_n + V} \right\} \{P_1 f_1(V) + P_2 f_2(V)\} \quad (31)$$

$$C' = \frac{(2 + \sqrt{\pi} \beta v_n) \sigma_s^{\text{max}}(v_\xi, 0)}{2\sigma_s^{\text{eff}}(v_n, T) \sqrt{\pi} \beta v_n} \quad (32)$$

$$v_\xi \in \left[ v_n - \frac{4}{\sqrt{\alpha}}, v_n + \frac{4}{\sqrt{\alpha}} \right] \quad (33)$$

$$\alpha = \frac{M_t}{2kT} \quad (34)$$

where  $\sigma_s^{\text{max}}(v_\xi, 0)$  is the maximum value of elastic scattering cross sections within a range of the dimensionless speed given by Eq. (33). The speed of the target is sampled from  $f_1(V)$  with probability

$P_1$  and from  $f_2(V)$  with probability  $P_2$ . The cosine of the azimuthal angle  $\mu$  is sampled uniformly over  $[-1, 1]$ . The ratios of  $v_r/(v_n + V)$  and  $\sigma_s(v_r, 0)/\sigma_s^{\max}(v_r, 0)$  in Eq. (19) come from two rejection tests applied to the sampled velocity of the target nucleus. The values of the two ratios are less than unity. The first rejection test is also included in the conventional free gas model and the second one is the additional rejection test in DBRC.

To implement the theory described above, several subroutines of the OpenMC code (Romano and Forget, 2013) are modified based on DBRC method for the cases where the incident neutron energy is from 0.4 eV to 210 eV. The modified OpenMC is used to generate the RI table for the subgroup method.

### 3. Numerical results

The continuous-energy nuclear data in ACE format used by the Monte Carlo method and the multi-group cross section nuclear data used by the subgroup method are generated based on the ENDF/B-VII.0. The RI tables for  $^{238}\text{U}$  and  $^{232}\text{Th}$  are prepared by OpenMC using both the conventional free gas scattering kernel and the DBRC. The RI tables of all the other resonant nuclides are prepared by RMET21 (Leszczynski, 1987) using the asymptotic scatter kernel. The use of RMET21 is to increase the efficiency for the calculations of the RI tables of the nuclides which have only slight resonance elastic scattering phenomenon. These RI tables are prepared for homogeneous systems.

The Dancoff correction, fast RIF scheme and DBRC are tested in isolation in Section 3.1, Section 3.2 and Section 3.3, respectively. Section 3.4 tests the FHR pebble problems when all the proposed corrections are included.

#### 3.1. Verification of the Dancoff correction

To test the scheme of treating double heterogeneity of the pebble sphere in the FHR, four cases are defined with different fuel. The dimensions of the TRISO particle and the pebble sphere are given in Tables 1 and 2, respectively. The nuclear densities of the fuel kernel are given in Table 3. The temperatures for the cases are given in Table 4. The number of TRISO particles embedded in the fuel zone of the pebble sphere is 15,000. Table 5 gives the reference eigenvalues calculated by OpenMC without DBRC and the errors of the eigenvalues calculated by SUGAR with three different calculation schemes. The first scheme considers only the first level heterogeneity of the pebble. The self-shielded cross sections are evaluated in a one-dimensional spherical shell model of TRISO particle with a white boundary. The second scheme considers only the second level heterogeneity. The fuel zone of the pebble is homogenized by volume and then the resonance calculation is performed based on the one-dimensional spherical shell model of the pebble. The last scheme carries out the Dancoff correction as described above. Moreover, the resonance interference is treated with the iteration scheme and the resonance elastic scattering correction is not applied for SUGAR. From Table 5 it can be observed that the errors of  $k_\infty$  are very large without considering the double

**Table 1**  
Dimensions of the TRISO particle.

Structure	Outer radius ( $\mu\text{m}$ )
Fuel kernel	500
Buffer	590
Inner pyro-carbon	630
Silicon carbide	665
Outer pyro-carbon	705

**Table 2**  
Dimensions of the pebble sphere.

Structure	Outer radius (cm)
Fuel zone	2.5
Pebble shell	3
Surrounding salt	3.54785

**Table 3**  
Atomic densities ( $10^{24}$  atom/cm<sup>3</sup>) of the fuel kernel.

	Cases 1 and 2	Cases 3 and 4
$^{238}\text{U}$	$2.12877 \times 10^{-2}$	0
$^{235}\text{U}$	$1.92585 \times 10^{-3}$	0
$^{233}\text{U}$	0	$1.92585 \times 10^{-3}$
$^{232}\text{Th}$	0	$2.12877 \times 10^{-2}$
$^{16}\text{O}$	$4.64272 \times 10^{-2}$	$4.64272 \times 10^{-2}$
$^{10}\text{B}$	$1.14694 \times 10^{-7}$	$1.14694 \times 10^{-7}$
$^{11}\text{B}$	$4.64570 \times 10^{-7}$	$4.64570 \times 10^{-7}$

**Table 4**  
Temperatures for the pebble sphere and surrounding salt.

	Case 1	Case 2	Case 3	Case 4
Pebble sphere	800	1000	800	1000
Salt	800	800	800	800

**Table 5**  
Comparison of  $k_\infty$  for the pebble problems with different calculation schemes.

Cases	Reference	Error/pcm		
		Scheme 1	Scheme 2	Scheme 3
Case 1	1.40216	2110	-6370	251
Case 2	1.38501	2270	-6450	350
Case 3	1.61411	1490	-1600	217
Case 4	1.61120	980	-1620	168

heterogeneity. SUGAR with the Dancoff correction predicts the eigenvalues within 500 pcm of errors compared to the reference.

#### 3.2. Comparison of resonance interference schemes

To isolate the resonance interference effect from the double heterogeneous effect, models of a single TRISO particle with different fuel are built and analyzed. The first case is a TRISO particle of  $\text{UO}_2$  fuel with enrichment 8.3%; the second case is a TRISO particle of  $\text{ThO}_2$  fuel with enrichment 8.3%; the third case is a TRISO with TRU fuel whose composition is given in Table 6. In the calculations, the reference self-shielded cross sections are calculated by OpenMC without DBRC. The RI table without considering resonance elastic scattering effect is applied in SUGAR. Four different schemes for treating the resonance interference effect are compared; that is, the conventional iteration scheme, the RNG

**Table 6**  
Compositions of the TRU.

Nuclide	Weight fraction (%)
$^{237}\text{Np}$	6.8
$^{238}\text{Pu}$	2.9
$^{239}\text{Pu}$	49.5
$^{240}\text{Pu}$	23.0
$^{241}\text{Pu}$	8.8
$^{242}\text{Pu}$	4.9
$^{241}\text{Am}$	2.8
$^{242\text{m}}\text{Am}$	0.02
$^{243}\text{Am}$	1.4

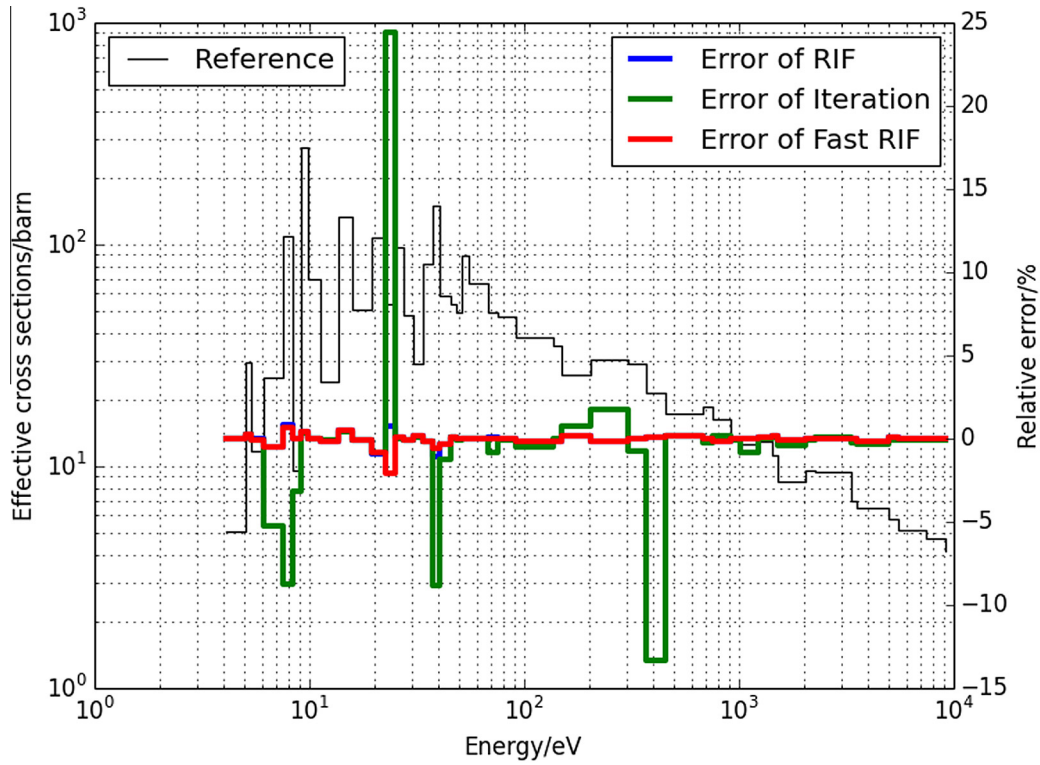


Fig. 2. Errors of effective absorption self-shielded cross section of different resonance interference schemes for  $^{235}\text{U}$  of case 1.

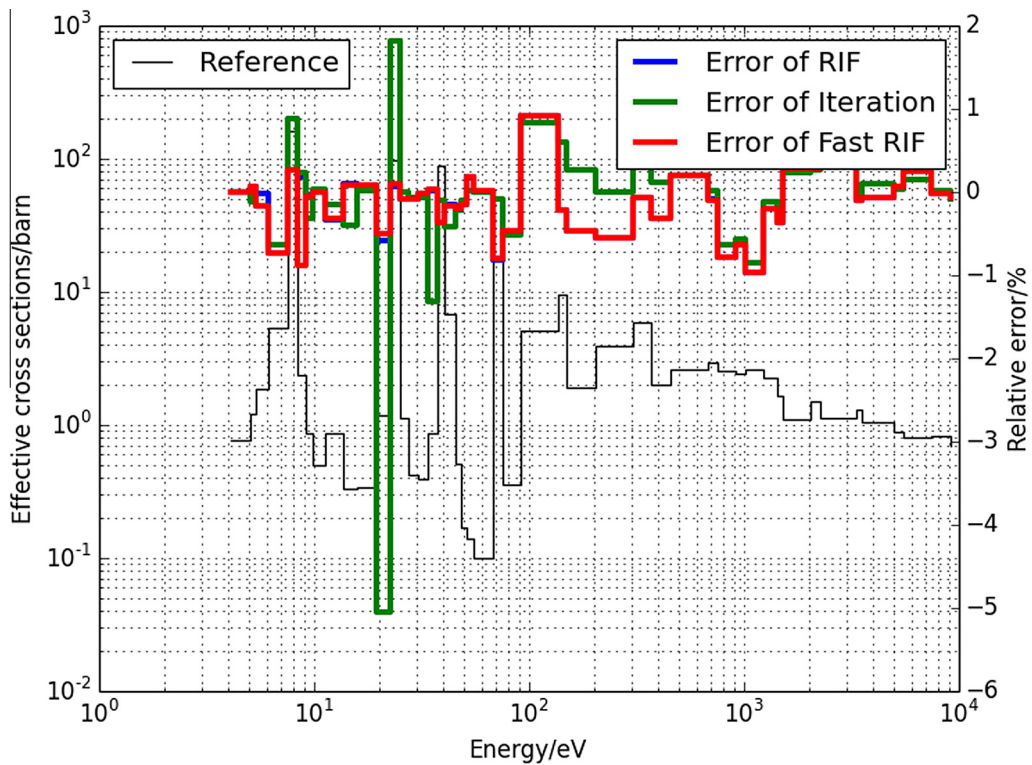


Fig. 3. Errors of effective absorption self-shielded cross section of different resonance interference schemes for  $^{238}\text{U}$  of case 1.

scheme, the conventional on-the-fly RIF scheme and the fast RIF scheme.

Figs. 2 and 3 provide a comparison of the self-shielded cross sections for the first case. Because the flux spectrum is mainly

determined by the dominant resonant nuclide  $^{238}\text{U}$ , the flux of the problem deviates little from the non-interfered flux used for generating RI table of  $^{238}\text{U}$  but significantly from that of  $^{235}\text{U}$ . Therefore, for the iteration scheme, the errors of the self-shielded

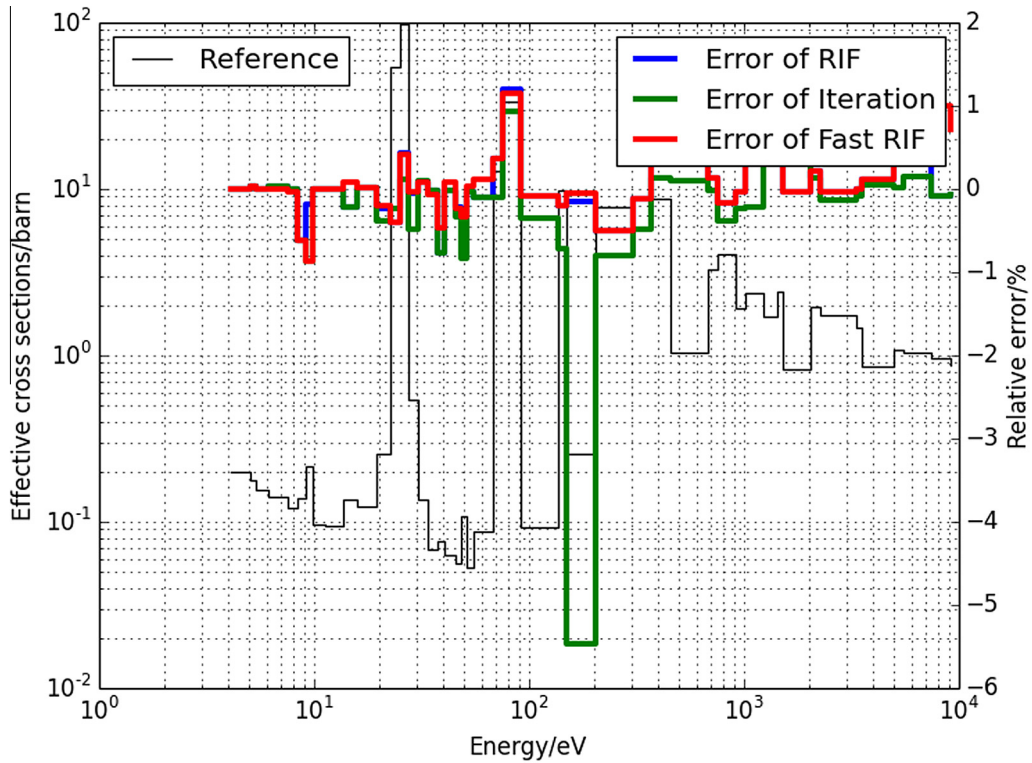


Fig. 4. Errors of effective absorption self-shielded cross section of different resonance interference schemes for  $^{232}\text{Th}$  of case 2.

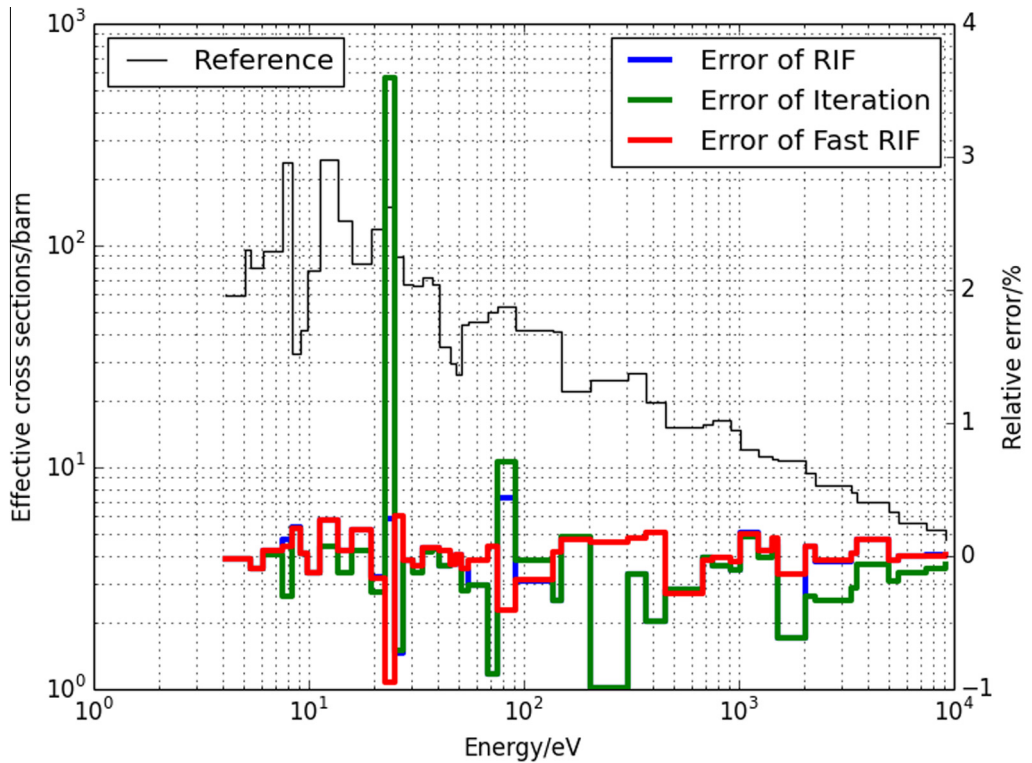


Fig. 5. Errors of effective absorption self-shielded cross section of different resonance interference schemes for  $^{233}\text{U}$  of case 2.

cross sections of  $^{235}\text{U}$  are larger than that of  $^{238}\text{U}$ . In the RIF and fast RIF scheme, the interference between  $^{235}\text{U}$  and  $^{238}\text{U}$  are considered by solving the continuous slowing down equations and the errors are reduced. The errors of the RIF and the fast RIF scheme are at

the same level. Figs. 4 and 5 give the results of the case 2. The RIF scheme and fast RIF again show an advantage over the iteration scheme in terms of errors of self-shielded cross sections. In the above two cases, since there are only two resonant nuclides in

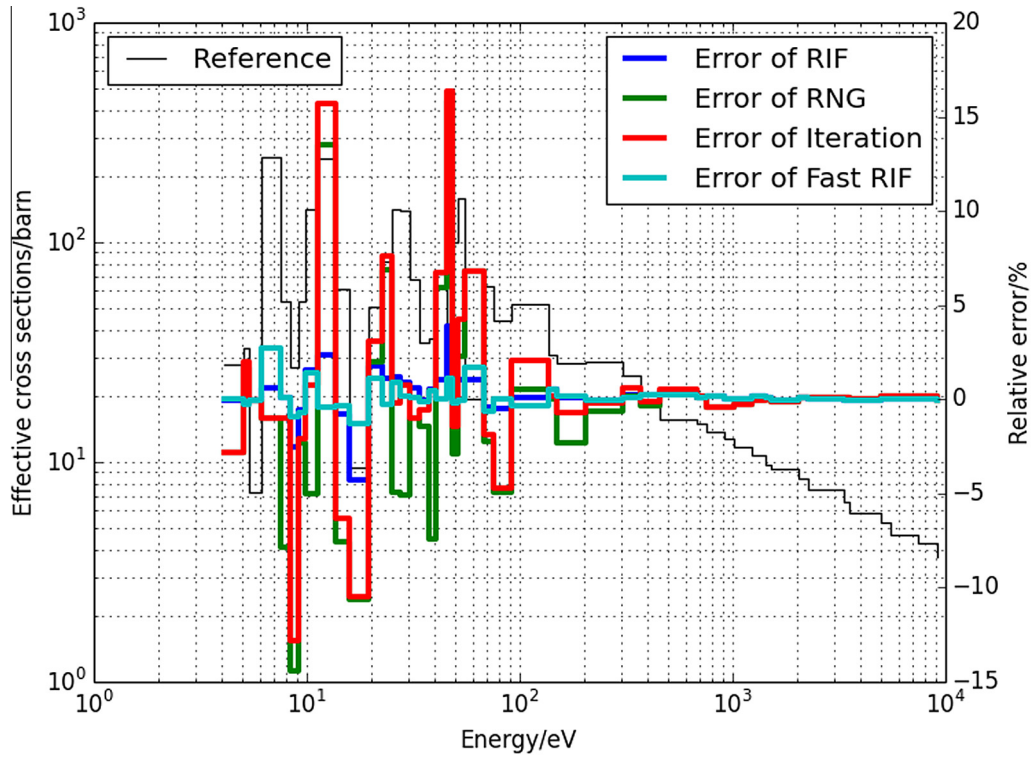


Fig. 6. Errors of effective absorption self-shielded cross section of different resonance interference schemes for  $^{237}\text{Np}$  of case 3.

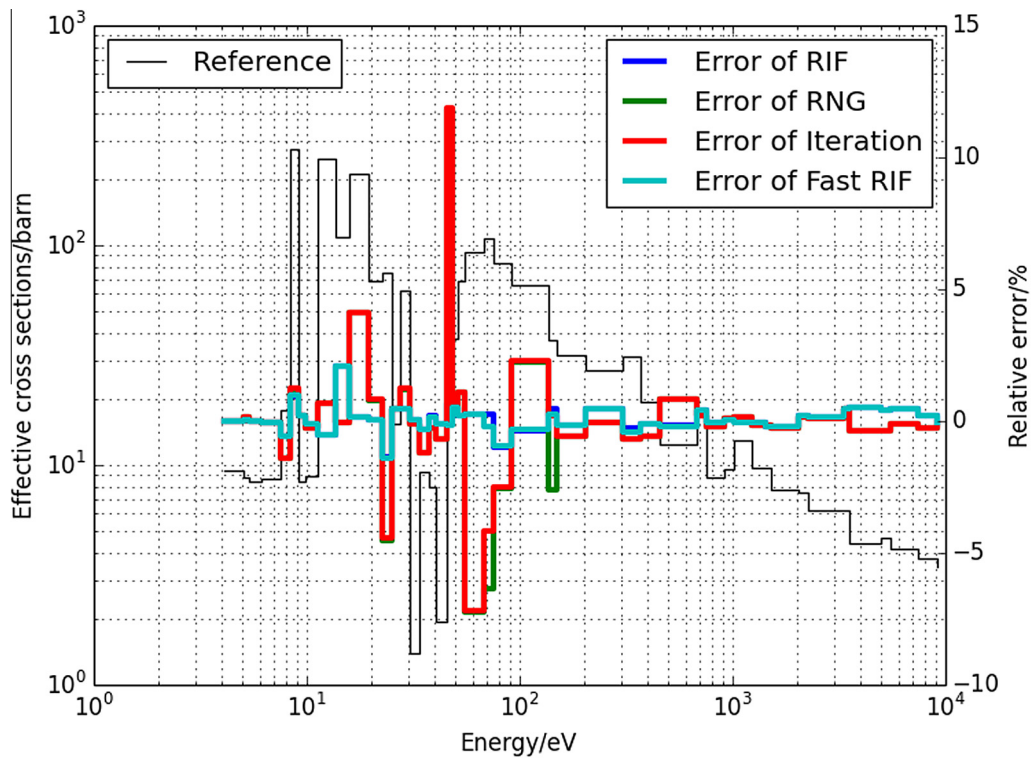


Fig. 7. Errors of effective absorption self-shielded cross section of different resonance interference schemes for  $^{239}\text{Pu}$  of case 3.

the fuel region, the RNG scheme is practically identical to the iteration scheme. The results of these two schemes are the same so that the results of the RNG scheme are not provided. Figs. 6, 7 and 8 show the errors of the self-shielded cross sections for case

3. Results for  $^{237}\text{Np}$ ,  $^{239}\text{Pu}$  and  $^{240}\text{Pu}$  are given and results for other resonant nuclides are similar. As shown in Fig. 6, the errors for  $^{237}\text{Np}$  of the iteration scheme are much larger than that for  $^{238}\text{U}$  in case 1 and  $^{232}\text{Th}$  in case 2 despite that it is the highest

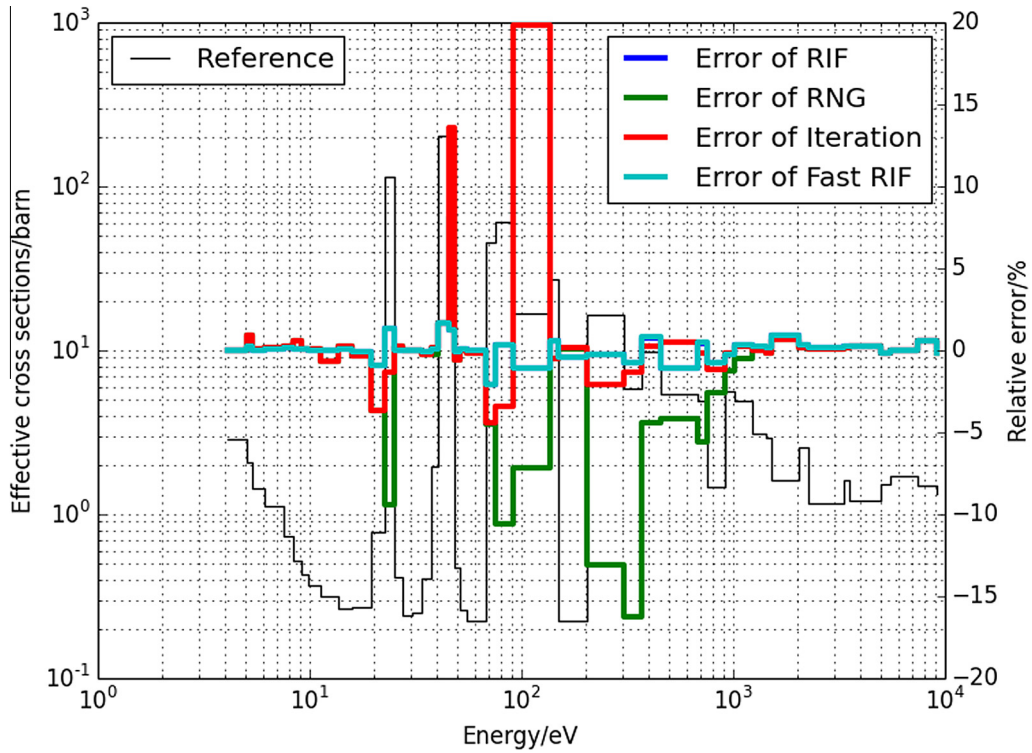


Fig. 8. Errors of effective absorption self-shielded cross section of different resonance interference schemes for <sup>240</sup>Pu of case 3.

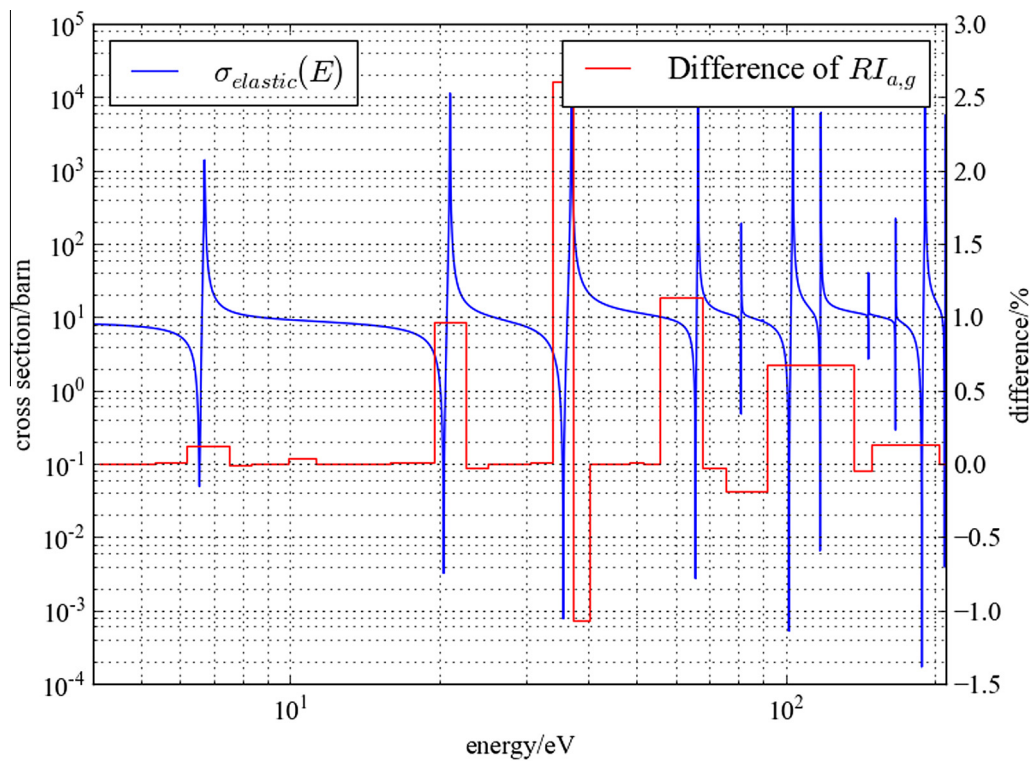


Fig. 9. Impact of resonance elastic scattering on absorption RI of <sup>238</sup>U.

composition. The compositions of the TRU are more balanced than that of the UO<sub>2</sub> and ThO<sub>2</sub> fuels. In addition, there are more resonant nuclides in TRU fuel. Therefore, the resonance interference effect is more significant than that in other two cases. The errors of the RNG scheme are also noticeable as it is based on the iteration scheme.

The results of the RIF and the fast RIF are in good agreement with the reference as in the previous two cases.

The CPU time required for the resonance calculation for case 3, including the time for the SFSP and the slowing down calculations, are compared in Table 7. Compared with the iteration scheme, the

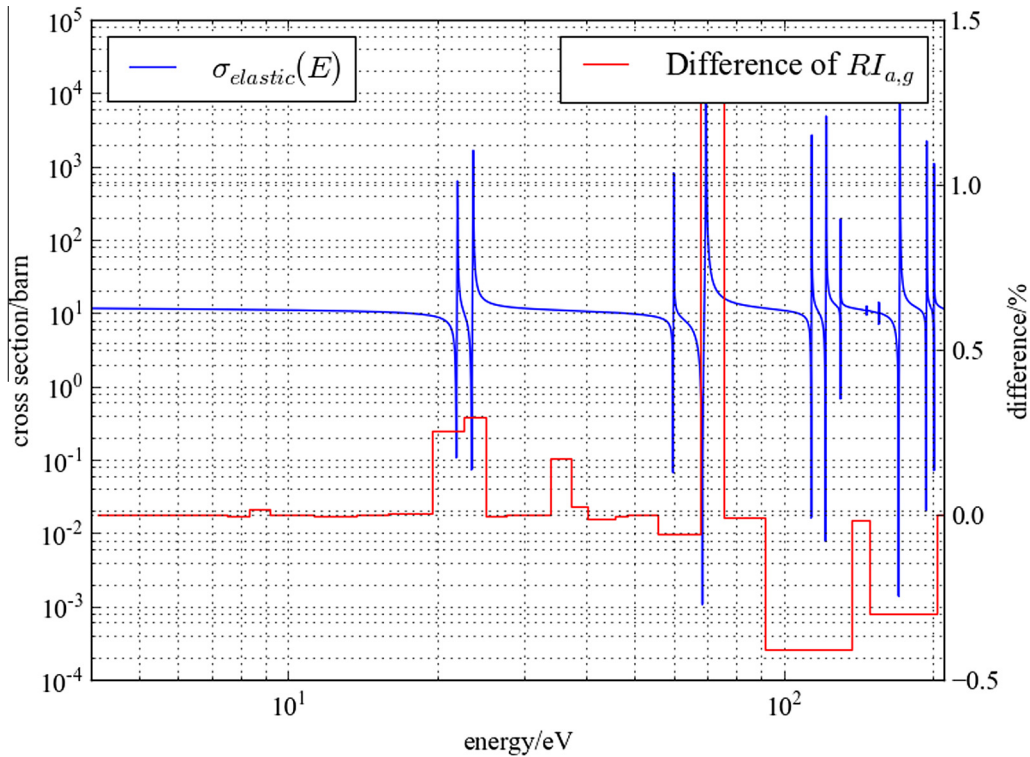


Fig. 10. Impact of resonance elastic scattering on absorption RI of  $^{232}\text{Th}$ .

**Table 7**  
Comparison of time for resonance calculation of TRISO with TRU fuel.

Scheme	SFSPs/n	Slowing down problems/n	Time for resonance calculation/s
Iteration	658	0	69.49
RNG	188	0	30.26
RIF	328	70	105.66
Fast RIF	47	10	31.87

RNG scheme groups the seven resonant nuclides into three categories and saves 56.45% of the resonance calculation time. The conventional RIF scheme need SFSP and slowing down calculations for each resonance nuclides, while the fast RIF scheme only need SFSP calculations for the dominant resonance nuclide and slowing down calculations for all the resonance nuclides for one time. The speed up ratio for the fast RIF scheme given by Eq. (20) is  $\sim 3.3$  compared with the conventional RIF scheme. In general, the iteration scheme and the conventional RIF scheme consumes the most time and the fast RIF scheme consumes the least.

**Table 8**  
Impact of resonance elastic scattering on  $k_{\infty}$  for  $\text{UO}_2$  pin cell problems at HZP of Mosteller benchmark.

Enrichment (%)	Impact of resonance elastic scattering on $k_{\infty}$ (pcm)				
	MVP-WCM	MCNP6-DBRC	TRIPOLI-DBRC	TRIPOLI-WCM	OpenMC-DBRC
0.711	-101	-9	-99	-115	-54
1.6	-	-74	-117	-135	-61
2.4	-91	-35	-100	-127	-78
3.1	-	-62	-98	-107	-53
3.9	-106	-70	-82	-110	-62
4.5	-	-38	-78	-95	-73
5.0	-82	-89	-88	-106	-79

### 3.3. Verification of the Doppler broadened scattering kernel

Firstly, to verify the correctness of the implementation of DBRC into OpenMC, the Mosteller Doppler defect benchmark (Mosteller, 2006) is analyzed with the modified OpenMC. The eigenvalues for  $\text{UO}_2$  pin cell problems at Hot Zero Power (HZP) and Hot Full Power (HFP) with the conventional scattering kernel and the DBRC are calculated. The differences in eigenvalues introduced by different scattering kernels are calculated and compared with those estimated in related research. The numerical results are given in Tables 8 and 9. The resonance elastic scattering effect is considered in MVP (Nagaya et al., 2005) via WCM (Mori and Nagaya, 2009), MCNP6 via DBRC (Sunny et al., 2012) and TRIPOLI via both (Zoia et al., 2013). The conclusion can be drawn that despite small discrepancies, these results obtained in this paper are consistent with those of other researchers in general. For the  $\text{UO}_2$  pin cell, the asymptotic scattering kernel overestimate the eigenvalue by tens of pcm to 140 pcm at HZP and 80 pcm to 230 pcm at HFP.

**Table 9**  
Impact of resonance elastic scattering on  $k_{\infty}$  for  $\text{UO}_2$  pin cell problems at HFP of Mosteller benchmark.

Enrichment (%)	Impact of resonance elastic scattering on $k_{\infty}$ (pcm)				
	MVP-WCM	MCNP6-DBRC	TRIPOLI-DBRC	TRIPOLI-WCM	OpenMC-DBRC
0.711	-180	-86	-186	-227	-162
1.6		-191	-171	-225	-169
2.4	-205	-150	-206	-220	-165
3.1		-133	-174	-204	-150
3.9	-182	-114	-178	-179	-137
4.5		-153	-175	-216	-148
5.0	-182	-119	-174	-189	-139

**Table 10**  
Eigenvalue errors of pebble with difference calculation schemes.

Cases	Reference	Errors/pcm				
		Scheme 1	Scheme 2	Scheme 3	Scheme 4	Scheme 5
Case 1	1.39892	2347	-6153	483	405	231
Case 2	1.38132	2542	-6204	618	497	252
Case 3	1.61411	1485	-1600	217	165	157
Case 4	1.61096	991	-1603	184	122	110

Scheme 1: Only considering first heterogeneity  
 Scheme 2: Only considering second heterogeneity  
 Scheme 3: Applying Dancoff correction to consider double heterogeneity  
 Scheme 4: Applying Dancoff correction and fast RIF  
 Scheme 5: Applying Dancoff correction, fast RIF and Doppler broadened scattering kernel

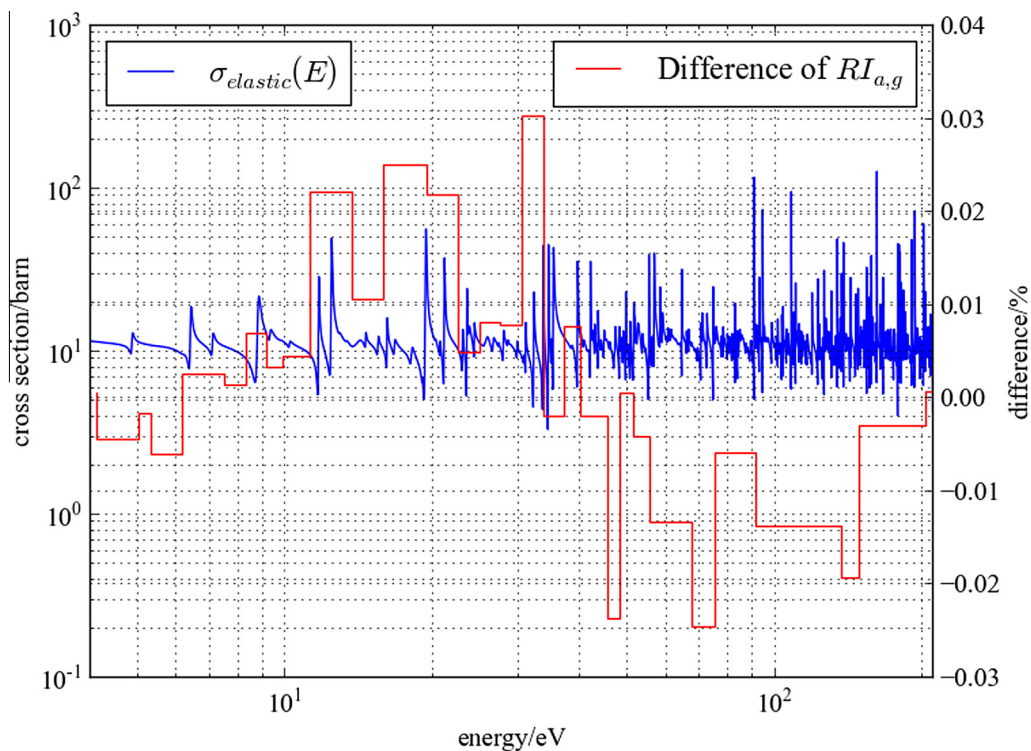


**Fig. 11.** Impact of resonance elastic scattering on absorption  $RI$  of  $^{235}\text{U}$ .

3.4. Tests of FHR pebble problems

The pebble problems described in Section 3.1 are calculated by different calculation schemes in SUGAR. The reference results are calculated by OpenMC with DBRC. The results and description of

these schemes are given in Table 10. The errors of schemes 1 and 2 are very large due to lack of considering double heterogeneity. The results of scheme 3 are much closer to the reference with Dancoff correction. The fast RIF correction improves the results to 50–120 pcm. The consideration of the Doppler broadened scattering

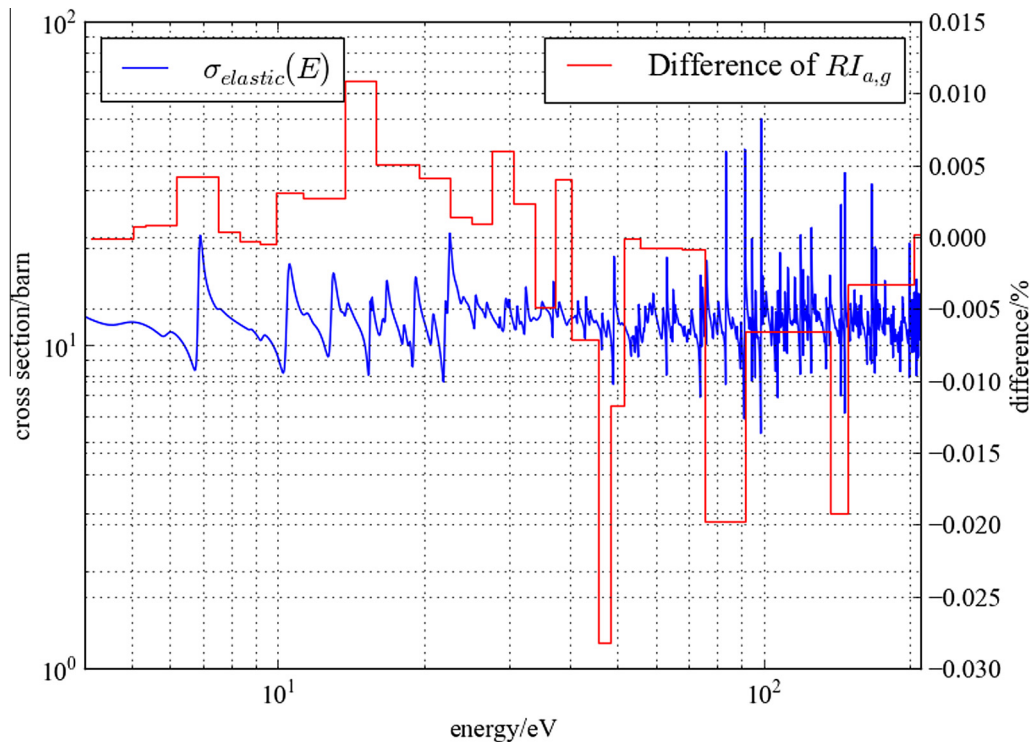


Fig. 12. Impact of resonance elastic scattering on absorption RI of  $^{233}\text{U}$ .

kernel brings a 150–250 pcm improvement for the pebbles with  $\text{UO}_2$  fuel while giving only a minor effect for  $\text{ThO}_2$  fuel. In order to elucidate the observation, the impact of the resonance elastic scattering on the absorption RI of each resonance nuclide in the homogeneous system at 1100 K with dilution to be 100 barn is shown in Figs. 9–12. The effect on the absorption RI of  $^{235}\text{U}$ ,  $^{233}\text{U}$  and  $^{232}\text{Th}$  is weak while the effect on the absorption RI of  $^{238}\text{U}$  is larger. Therefore resonance elastic scattering has a relatively larger effect on the eigenvalues of pebbles with  $\text{UO}_2$  fuel.

#### 4. Conclusions

In order to address the challenges brought about by the new design features of the FHR, the subgroup method is improved in three aspects.

Firstly, to treat the double heterogeneity, the Dancoff correction is applied in the subgroup method. The errors of the eigenvalues calculated by the subgroup method with the Dancoff correction scheme are within 500 pcm.

Secondly, the fast RIF scheme is proposed to treat the resonance interference effect. Four schemes to treat the resonance interference effect are compared. The RIF schemes, including the fast RIF and the conventional RIF, obtain higher precision than the iteration scheme and the RNG scheme. Compared with the iteration scheme, the RNG scheme saves 56.45% of the computation time for the TRU TRISO if the resonant nuclides are grouped into three categories. The accuracy of the fast RIF and the conventional RIF is at the same level. Compared with the conventional on-the-fly RIF scheme, the speed up ratio of the fast RIF scheme is  $\sim 3.3$  for TRU TRISO. With fast RIF correction, the eigenvalues of the pebble problems are improved by 50–120 pcm.

Finally, to take into account the resonance elastic scattering effect, the OpenMC code is modified via DBRC method and is used to generate RI tables for the subgroup method. The Mosteller benchmark problems are analyzed with the modified OpenMC

code. The results show that the Doppler broadened scattering kernel decreases  $\sim 200$  pcm in eigenvalues for LWR pin cell problems at HFP which is consistent with those found in the literature. For pebbles with  $\text{UO}_2$  fuel, consideration of the Doppler broadened scattering kernel improves results to the extent of 150–250 pcm; while for pebbles with  $\text{ThO}_2$  fuel, as the resonance elastic scattering effect is much weaker, the improvement of this correction is minor. With all these three corrections, the subgroup method predicts eigenvalues within 300 pcm of errors compared with the reference.

#### Acknowledgement

This work is financially supported by the National Natural Science Foundation of China (Nos. 91126005 and 91226106) and Science and Technology on Reactor System Design Technology Laboratory. The authors would like to thank Professor Barry D. Ganapol from the University of Arizona for valuable discussions and his revisions to this paper.

#### References

- Askew, J.R., Fayers, F.J., Kemshell, P.B., 1966. A general description of lattice code WIMS. *J. Brit. Nucl. Energy Soc.* 5, 546–585.
- Becker, B., Dagan, R., Broeders, C.H.M., Lohnert, G.H., 2009a. Improvement of the resonance scattering treatment in MCNP in view of HTR calculations. *Ann. Nucl. Energy* 36, 281–285.
- Becker, B., Dagan, R., Lohnert, G., 2009b. Proof and implementation of the stochastic formula for ideal gas, energy dependent scattering kernel. *Ann. Nucl. Energy* 36, 470–474.
- Bende, E.E., Hogenbirk, A.H., 1999. Analytical calculation of the average Dancoff factor for a fuel kernel in a pebble bed high-temperature reactor. *Nucl. Sci. Eng.* 133, 147–162.
- Cao, L., Wu, H., Liu, Q., Chen, Q., 2011. Arbitrary geometry resonance calculation using subgroup method and method of characteristics. In: M&C 2011, Rio de Janeiro, RJ, Brazil, May 8–12, 2011, on CD-ROM.
- Chen, Q., Wu, H., Cao, L., 2008. Auto MOC—A 2D neutron transport code for arbitrary geometry based on the method of characteristics and customization of AutoCAD. *Nucl. Eng. Des.* 238, 2828–2833.

- Chiba, G., 2003. A combined method to evaluate the resonance self shielding effect in power fast reactor fuel assembly calculation. *J. Nucl. Sci. Technol.* 40, 537–543.
- Chiba, G., Unesaki, H., 2006. Improvement of moment-based probability table for resonance self-shielding calculation. *Ann. Nucl. Energy* 33, 1141–1146.
- Engle, W.W., 1967. A user's manual for ANISN: a one dimensional discrete ordinates transport code with anisotropic scattering. Union Carbide Corporation, Nuclear Division, Oak Ridge Gaseous Diffusion Plant.
- Fratoni, M., 2008. Development and Application of Methodologies for the Neutronic Design of the Pebble Bed Advanced High Temperature Reactor (PB-AHTR). University of California, Berkeley.
- He, L., Wu, H., Cao, L., Li, Y., 2014. Improvements of the subgroup resonance calculation code SUGAR. *Ann. Nucl. Energy* 66, 5–12.
- Hébert, A., 2009. Development of the subgroup projection method for resonance self-shielding calculations. *Nucl. Sci. Eng.* 162, 56–75.
- Hyun, S., Kim, H., Man, J., Kyung, J., 2010. An evaluation of Dancoff factor for pebble-type reactor using Monte Carlo method. In: Proceedings of ICAPP, San Diego, CA, USA, June 13–17, 2010.
- Ishiguro, Y., Takano, H., 1971. PEACO: a code for calculation of group constant of resonance energy region in heterogeneous systems.
- Joo, H.G., Cho, J.Y., Kim, K.S., Lee, C.C., Zee, S.Q., 2004. Methods and performance of a three-dimensional whole-core transport code DeCART. In: PHYSOR 2004, Chicago, Illinois, April 25–29, 2004, on CD-ROM. pp. 21–34.
- Joo, H.G., Kim, G.Y., Pogobekyan, L., 2009. Subgroup weight generation based on shielded pin-cell cross section conservation. *Ann. Nucl. Energy* 36, 859–868.
- Kidman, R.B., Lindenmeier, Clark W., Schenter, R.E., 1970. Resonance Cross Shielding in Reactor Analysis. Pacific Northwest Laboratory, Richland Wash.
- Kim, Y., Hartanto, D., 2012. A high-fidelity Monte Carlo evaluation of CANDU-6 safety parameters. In: PHYSOR 2012, Knoxville, Tennessee, USA, April 15–20, 2012, on CD-ROM.
- Kim, K.S., Hong, S.G., 2011. A new procedure to generate resonance integral table with an explicit resonance interference for transport lattice codes. *Ann. Nucl. Energy* 38, 118–127.
- Kim, K., Williams, M.L., 2012. Preliminary assessment of resonance interference consideration by using 0-D slowing down calculation in the embedded self-shielding method. In: ANS Winter Meeting and Nuclear Technology Expo, San Diego, CA, USA, 2012.
- Kim, K.-S., Lee, C.C., Chang, M.H., Zee, S.Q., 2003. Monte Carlo resonance treatment for the deterministic transport lattice code. *J. Korean Phys. Soc.*
- Kloosterman, J.L., Ougouag, A.M., 2007. Comparison and extension of Dancoff factors for pebble-bed reactors. *Nucl. Sci. Eng.* 157, 16–29.
- Kloosterman, J.L., Ougouag, A.M., Falls, I., 2005. Spatial effects in Dancoff factor calculations for pebble-bed HTRs. In: M&C 2005, Avignon, France, September 12–15, 2005, on CD-ROM.
- Lee, D., Smith, K., Rhodes, J., 2008. The impact of 238U resonance elastic scattering approximations on thermal reactor Doppler reactivity. In: PHYSOR 2008, Interlaken, Switzerland, September 14–19, 2008.
- Leszczynski, F., 1987. Neutron resonance treatment with details in space and energy for pin cells and rod clusters. *Ann. Nucl. Energy* 14, 589–601.
- Li, X.X., Cai, X.Z., Jiang, D.Z., Ma, Y.W., Huang, J.F., Zou, C.Y., Yu, C.G., Han, J.L., Chen, J.G., 2015. Analysis of thorium and uranium based nuclear fuel options in Fluoride salt-cooled High-temperature Reactor. *Prog. Nucl. Energy* 78, 285–290.
- Liu, Y., Collins, B., Kochunas, B., Martin, W., Kim, K., Williams, M., 2013a. Resonance self-shielding methodology in MPACT. In: M&C 2013, Sun Valley, Idaho, May 5–9, 2013, on CD-ROM. pp. 580–592.
- Liu, Y., Martin, W.R., Kim, K.S., Williams, M.L., 2013b. Modeling resonance interference by 0-D slowing-down solution with embedded self-shielding method. In: M&C 2013, Sun Valley, Idaho, May 5–9, 2013, on CD-ROM. pp. 160–174.
- MacFarlane, R.E., 2000. NJOY99.0: a code system for producing pointwise and multigroup neutron and photon cross sections from ENDF/B evaluated nuclear data.
- Mao, L., Sanchez, R., Zmijarevic, I., 2015. Considering the up-scattering in resonance interference treatment in APOLLO3. In: ANS M&C 2015, Nashville, Tennessee, April 19–23, 2015, on CD-ROM.
- Mori, T., Nagaya, Y., 2009. Comparison of resonance elastic scattering models newly implemented in MVP continuous-energy Monte Carlo code. *J. Nucl. Sci. Technol.* 46, 793–798.
- Mosteller, R.D., 2006. Computational benchmarks for the Doppler reactivity defect. Nagaya, Y., Okumura, K., Mori, T., Nakagawa, M., 2005. MVP/GMVP II: general purpose Monte Carlo codes for neutron and photon transport calculations based on continuous energy and multigroup methods.
- Nikolaev, M.N., Ignatov, A.A., Isaev, N.V., Khokhlov, V.F., 1971. The method of subgroups for considering the resonance structure of cross sections in neutron calculations. *Sov. At. Energy* 30, 528–533.
- Ono, M., WADA, K., Kitada, T., 2012. Simplified treatment of exact resonance elastic scattering model in deterministic slowing down equation. In: PHYSOR 2012, Knoxville, Tennessee, USA, April 15–20, 2012, on CD-ROM.
- Ouisloumen, M., Sanchez, R., 1991. A model for neutron scattering off heavy isotopes that accounts for thermal agitation effects. *Nucl. Sci. Eng.* 107, 189–200.
- Peng, S., Jiang, X., Zhang, S., Wang, D., 2013. Subgroup method with resonance interference factor table. *Ann. Nucl. Energy* 59, 176–187.
- Romano, P.K., Forget, B., 2013. The OpenMC Monte Carlo particle transport code. *Ann. Nucl. Energy* 51, 274–281.
- Sanchez, R., Masiello, E., 2002. Treatment of the double heterogeneity with the method of characteristics. In: PHYSOR 2002, Seoul, Korea, October 7–10, 2002.
- Stamm'ler, R.J.J., 2001. HELIOS methods. Studsvik Scandpower.
- Sunny, E.E., Brown, F.B., Kiedrowski, B.C., Martin, W.R., 2012. Temperature effects of resonance scattering for epithermal neutrons in MCNP. In: PHYSOR 2012, Knoxville, Tennessee, USA, April 15–20, 2012, on CD-ROM. pp. 1–9.
- Talamo, A., 2007. Analytical calculation of the average Dancoff factor for prismatic high-temperature reactors. *Nucl. Sci. Eng.* 156, 343–356.
- Tsuchihashi, K., Ishiguro, Y., Kaneko, K., 1985. Double heterogeneity effect on resonance absorption in very high temperature gas-cooled reactor. *J. Nucl. Sci. Technol.* 22, 16–27.
- Wehlage, E., Knott, D., Mills, V.W., 2005. Modeling resonance interference effects in the lattice physics code LANCER02. In: M&C 2005, Avignon, France, September 12–15, 2005, on CD-ROM.
- Williams, M.L., 1983. Correction of multigroup cross sections for resolved resonance interference in mixed absorbers. *Nucl. Sci. Eng.* 83, 37–49.
- X-5 Monte Carlo Team, 2003. MCNP – a general Monte Carlo n-particle transport code, version 5.
- Zhang, H., Wu, H., Cao, L., 2011. An acceleration technique for 2D MOC based on Krylov subspace and domain decomposition methods. *Ann. Nucl. Energy* 38, 2742–2751.
- Zoia, A., Brun, E., Jouanne, C., Malvagi, F., 2013. Doppler broadening of neutron elastic scattering kernel in Tripoli-4<sup>®</sup>. *Ann. Nucl. Energy* 54, 218–226.